

## SUPPLEMENTARY FIGURE LEGENDS

### Supplementary Fig. 1. Tandem mass spectra of ATM phosphopeptides reveal new human and mouse phosphorylation sites.

Titanium dioxide phosphopeptide enriched tryptic digests of human or mouse ATM were analysed by LC-MS/MS in multiple ion monitoring mode (see Methods). Spectra across the eluting phosphopeptide peaks were combined to improve the signal to noise ratio. The signal intensity for each ion is a measure of the average absolute counts for each ion. **A. Mass spectrum of phosphorylated hATM 1883-1898.** The triply charged precursor ion was at m/z 639.9. The phospho-T1885 was observed between the b2 and b3 ions and the y13 and y14 ions. **B. Mass spectrum of phosphorylated mATM 1889-1904.** The doubly charged precursor ion was at m/z 902.9. The spectrum was a mixture of two mono-phosphopeptides. Phospho-T1891 was observed between the b2 and b3 ions and the y13 and y14 ions. Ions specific to this phosphopeptide are shown in red. Phospho-S1899 was observed between the y5 and y6 ions. Ions specific to this phosphopeptide are shown in blue. These latter ions were much more abundant than the ions for the phospho-T1891 sequence. Therefore, it is likely that phosphorylation at S1899 was more abundant than phosphorylation at T1891. **C. Mass spectrum of phosphorylated mATM 363-374.** The doubly charged precursor ion was at m/z 738.9. Phospho-S367 was observed between the y7 and y8 ions. **D. Mass spectrum of phosphorylated mATM 1980-1988.** The doubly charged precursor ion was at m/z 1033.0. Phospho-T1987 was observed between the y11 and y12 ions. **E. Mass spectrum of phosphorylated mATM 3003-3014.** The doubly charged precursor ion was at m/z 725.3. Phospho-T3006 was deduced as the only possible phosphorylation site between the y7 and y9 ions or b2 and b4 ions. **F. Mass spectrum of phosphorylated hATM 2994-3004 with the D3003→N polymorphism.** The doubly charged precursor ion was at m/z 680.8. Phospho-S2996, found previously by Daub et al (49), was observed between the y8 and y9 ions.

### Supplementary Fig. 2. Specificity of the pS367-ATM and pS2996-ATM antibodies.

**A.** The phosphopeptides containing pS367, pS1893 and pS1981 and unphosphorylated peptides were blotted onto nitrocellulose membranes (Hybond ECL, 0.2 $\mu$ M, Amersham Biosciences), at 250ng and 500ng. The membranes were incubated with affinity-purified rabbit pS367-ATM antibody, antibody specifically recognised the corresponding phosphopeptide. Antibody did not recognise the unphosphorylated peptides.

**B.** The phosphopeptides containing pS2996 and pS1981 and unphosphorylated peptides were spotted onto nitrocellulose membranes (Hybond ECL, 0.2 $\mu$ M, Amersham Biosciences), at 250ng and 500ng. The membranes were incubated with affinity-purified rabbit pS2996-ATM antibody, antibody specifically recognised the corresponding phosphopeptide. Antibody did not recognise the unphosphorylated peptides.

### Supplementary Fig. 3. Localization of ATM pS367 to sites of DNA damage.

Normal human diploid fibroblasts (HE49) were exposed to 1Gy of X-irradiation, fixed after 1 hr incubation and stained for pS367, pS1981,  $\gamma$ H2AX and 53BP1. DNA damage-induced foci were visualized by immunofluorescence microscopy. Co-localization of pS367 and pS1981 ATM was evident, as well as co-localization of pS367 ATM with  $\gamma$ H2AX and 53BP1.

### Supplementary Fig. 4. Recruitment of ATM kinase phosphorylated at S1981 to the sites of DNA damage induced by heavy ions.

AG1522D human fibroblasts were subjected to the beam of Xe ions (LET of 8800 keV/ $\mu$ m). Cells were fixed at the indicated time points after irradiation and immunofluorescence microscopy was performed with antibodies to **A** ATM and  $\gamma$ -H2AX proteins and **B** ATM pS1981 and  $\gamma$ H2AX. DNA was visualized with TOPRO3 stain.

### Supplementary Fig. 5. Recruitment of ATM kinase phosphorylated at S367 to the sites of DNA damage induced by irradiation with $^{12}\text{C}$ and $^{64}\text{Ni}$ ions.

**A.** AG1522D human fibroblasts were subjected to a beam of  $^{12}\text{C}$  ions (LET 170 keV/  $\mu$ m). Cells were fixed 10 min after irradiation and immunofluorescence microscopy was performed with

antibodies to pS367 ATM and pS1981 ATM proteins. DNA was visualized with TOPRO3 stain. **B.** AG1522D human fibroblasts were subjected to a beam of  $^{64}\text{Ni}$  ions (LET 3430 keV/  $\mu\text{m}$ ), fixed 1 h after irradiation and processed as described in A.

**Supplementary Fig. 6. Recruitment of ATM kinase phosphorylated at S367 to the sites of DNA damage induced by irradiation with  $^{64}\text{Ni}$  ions in Nbs cells.**

AG1522D and Nbs human fibroblasts were subjected to a beam of  $^{64}\text{Ni}$  ions (LET 3430 keV/  $\mu\text{m}$ ). Cells were fixed 1 hr after irradiation and immunofluorescence microscopy was performed with antibodies to **A.** pS1981 ATM and **B.** pS367 ATM proteins. DNA was visualized with TOPRO3 stain.

**Supplementary Figure 7 Time-lapse imaging of YFP-ATM expressing HeLa cells before and after irradiation with  $^{56}\text{Fe}$  ions.**

**A.** Living cells were imaged before irradiation and first 7 min after irradiation with iron ions. An example of cells expressing YFP-ATMwt is shown. Recruitment of YFP-ATM to the sites of damage produced by heavy ions is visualized in real time as white dots (foci) appearing in the nucleus. Images were recorded at 20 s intervals. **B.** Kinetics of ATM vs S367A ATM accumulation at the sites of DNA damage induced by iron ions irradiation. n=6 for YFP-ATM wt, n=4 for YFP-S367A and YFP-S1981.

**Supplementary Figure 8 Time-lapse imaging of YFP-ATM S2996A expressing A-T cells before and after irradiation with  $^{197}\text{Au}$  ions.**

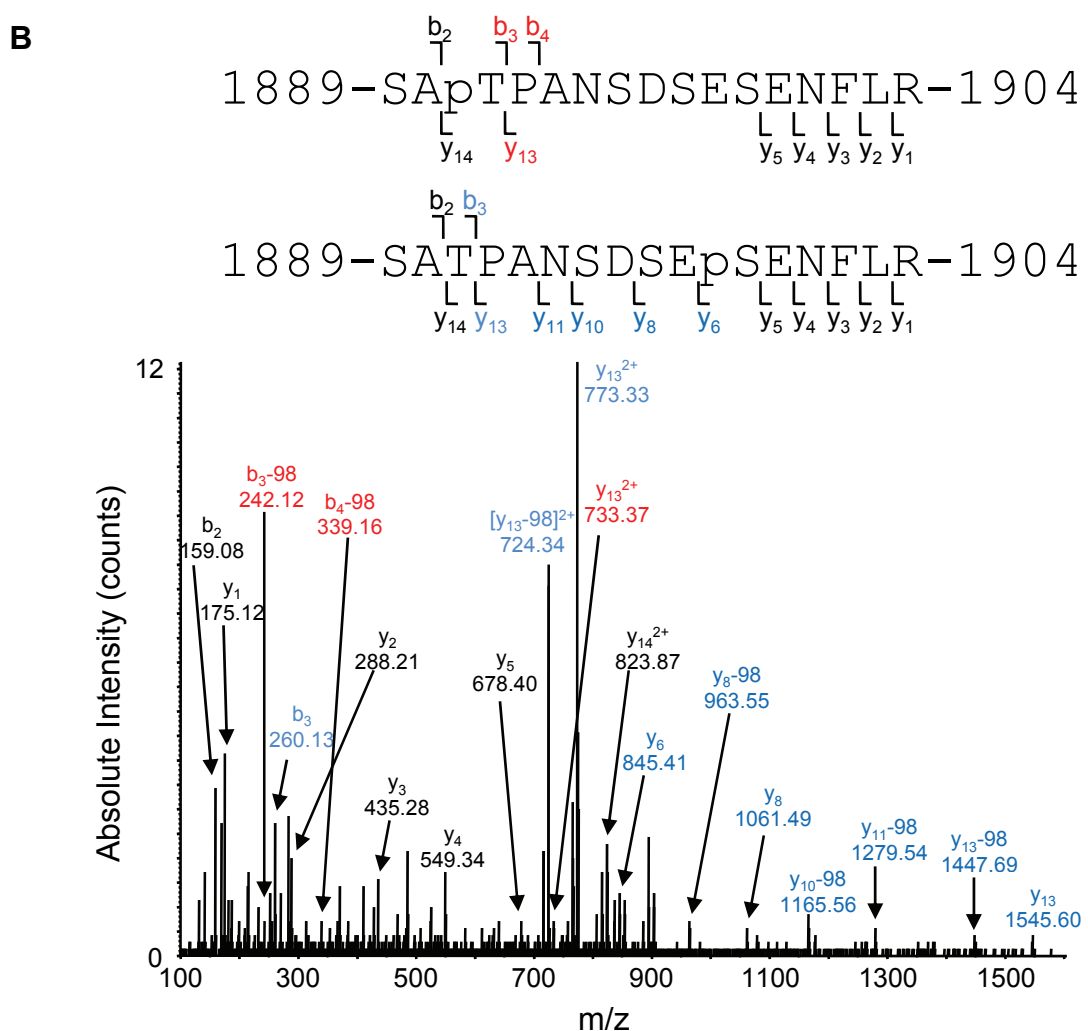
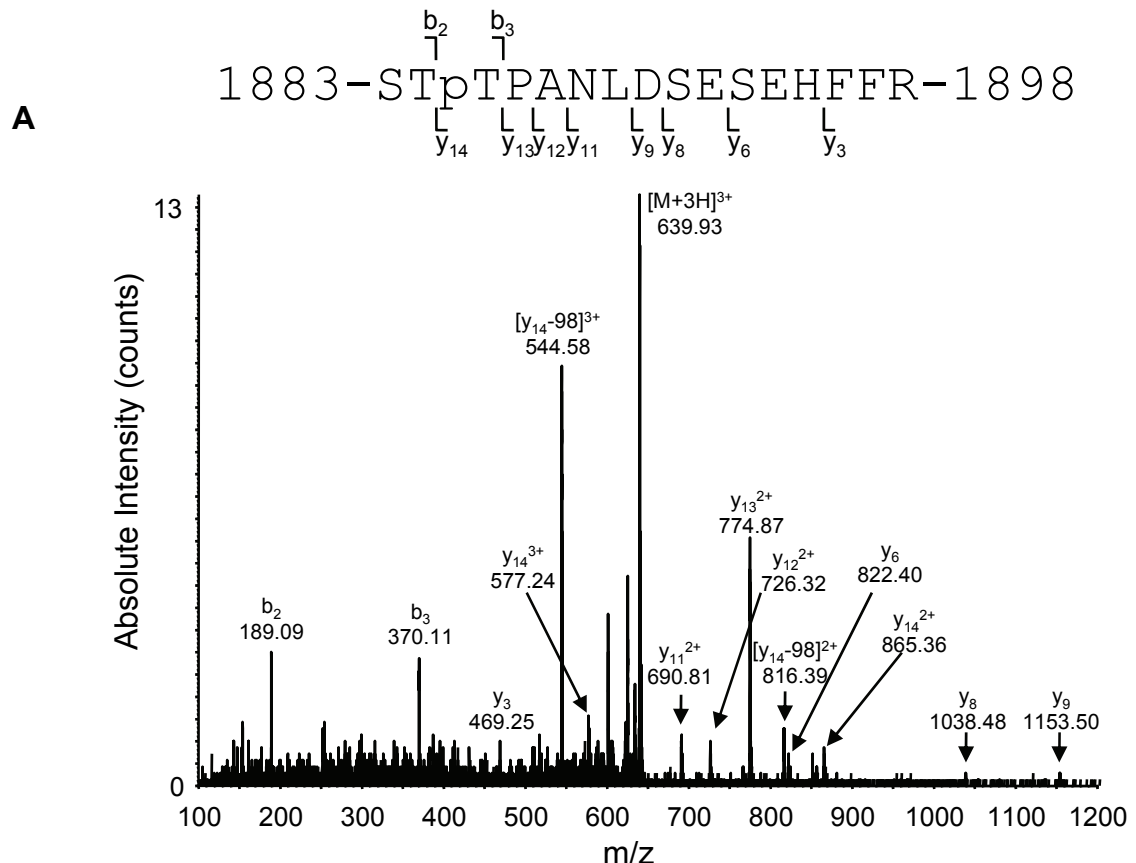
Kinetics of wt ATM vs S2996A ATM accumulation at the sites of DNA damage induced by irradiation with gold ions. The error bars represent the 95% confidence interval of the mean; n= 6 for YFP-ATM wt and n= 12 for YFP-ATM S2996A.

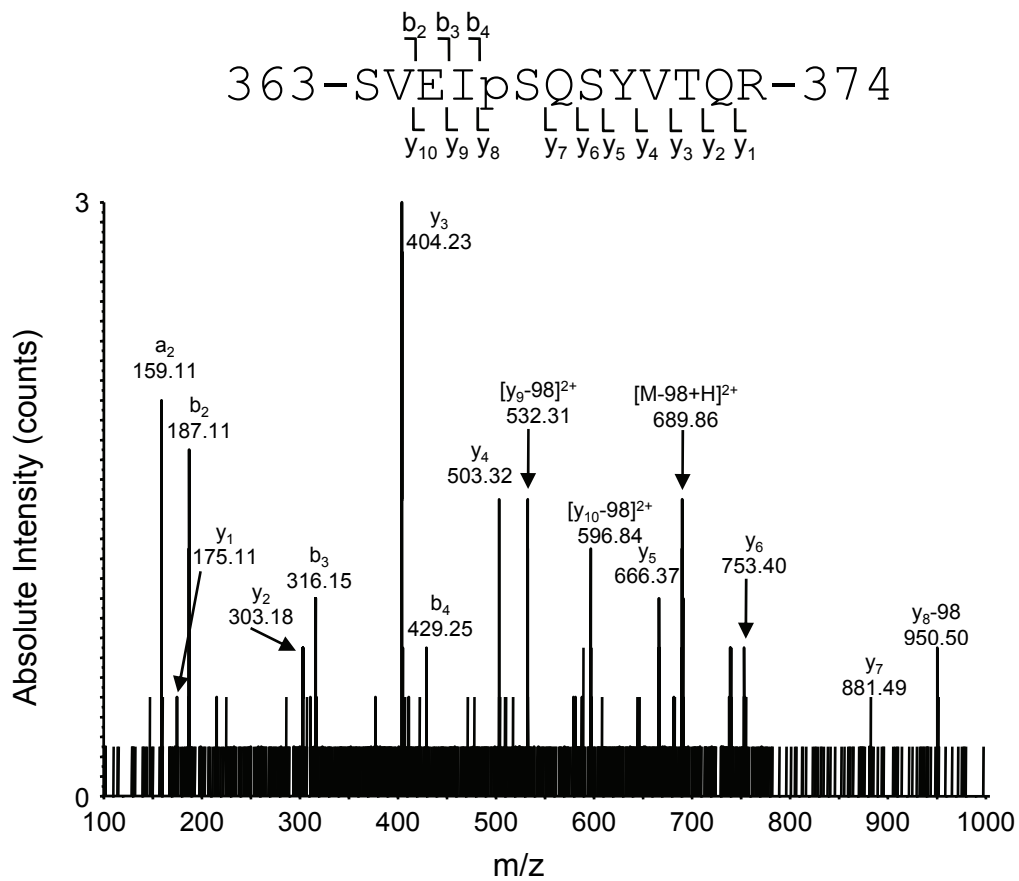
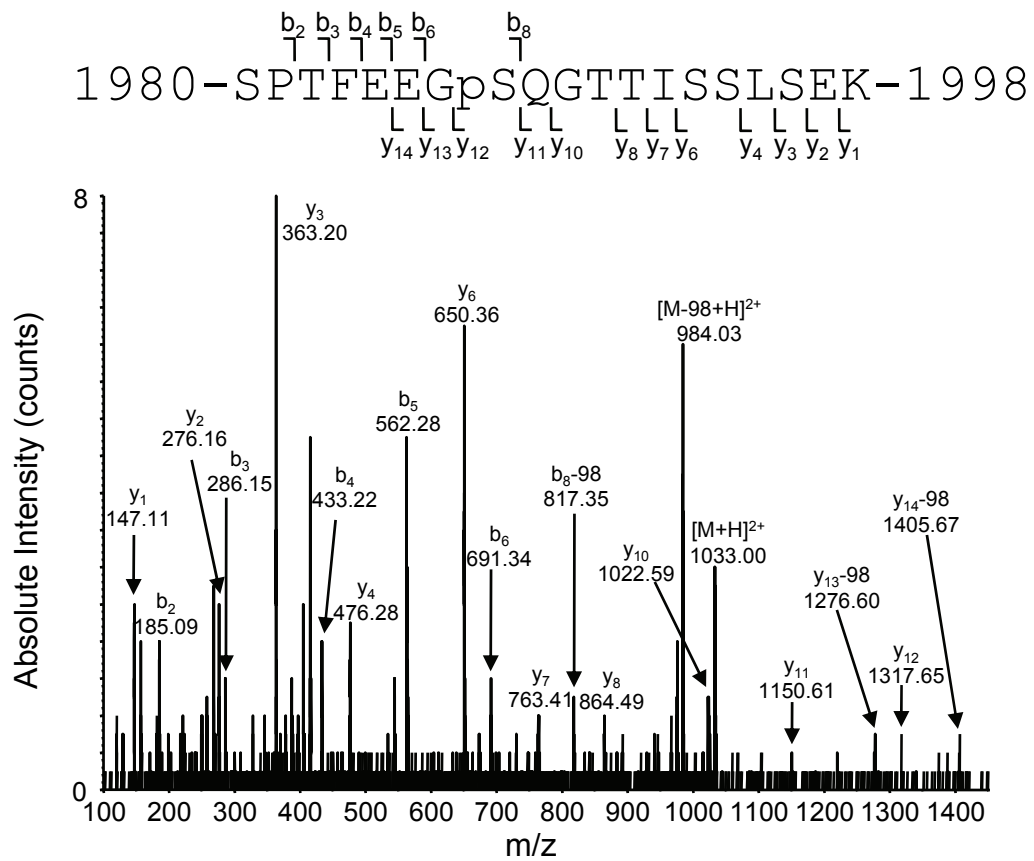
**Supplementary Figure 9. ATM autophosphorylation site mutants S1981A and S2996A fail to correct radiosensitivity of A-T cells. A.** Survival of control (C35ABR), AT1ABR and AT1ABR cells transfected with pMAT1, S2996A and S1981A mutant forms of ATM. Cells were induced with CdCl<sub>2</sub> for 16 hrs, exposed to radiation over the range 0-4 Gy and incubated for 3 days, prior to cell counting and determination of cell survival. Survival is expressed as a percentage of radiated/unirradiated. An average of triplicate experiments is shown for each point. Error bars represent SEM. **B.** Expression levels of ATM wt (pMAT1), S2996A and S1981A ATM proteins after 16 hr induction with 5  $\mu\text{M}$  CdCl<sub>2</sub>.

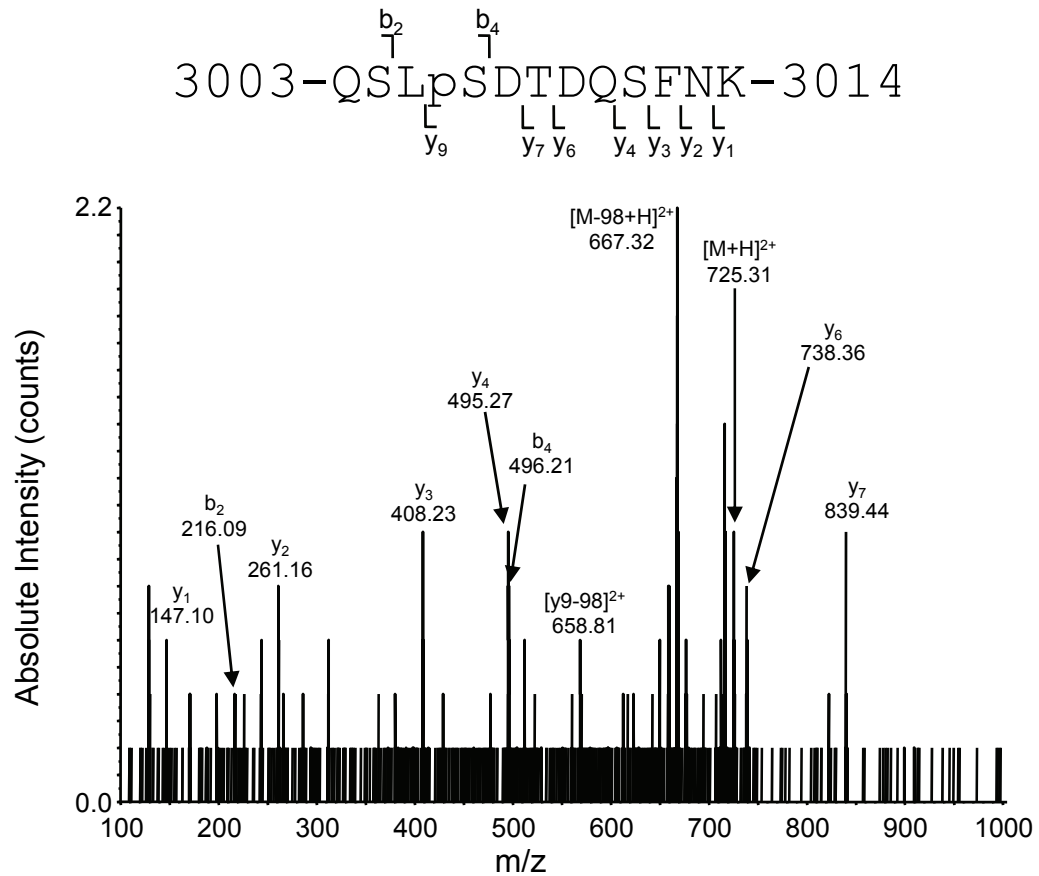
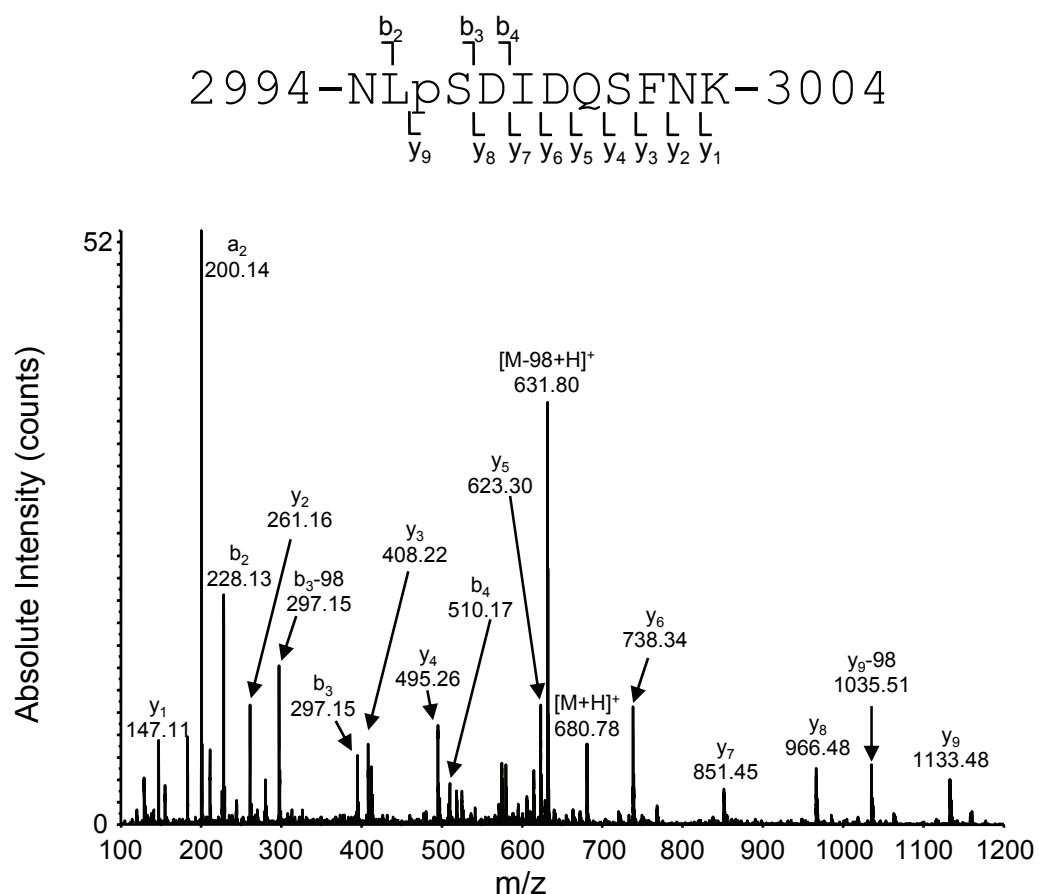
**Supplementary Table 1: Summary of Phosphorylation sites identified in ATM**

Sequence	Number of Sites	Phosphorylation Site
KEpTECLRIAKPNVSApSpTQASR	3	pT <sup>72</sup> E <sup>1</sup> pS <sup>85</sup> T <sup>1</sup> pT <sup>86</sup> Q <sup>1</sup>
SLEIp <u>S</u> QSYTTpTQR	2	pS <sup>367</sup> Q <sup>1,2</sup> pT <sup>373</sup> Q <sup>1</sup>
KKp <u>S</u> PNKI	1	pS <sup>794</sup> P <sup>5</sup>
pSTpTPANLDSE <u>p</u> SEHFFR	3	pS <sup>1883</sup> T <sup>5</sup> pT <sup>1885</sup> P <sup>6</sup> pS <sup>1893</sup> E <sup>2</sup>
SLAFEEG <u>p</u> SQSTpTISSLSEK	2	pS <sup>1981</sup> Q <sup>1,2,3,4</sup> pT <sup>1985</sup> I <sup>1</sup>
GHSFWEIpYKMTTDPM	1	pY <sup>1753</sup> K <sup>5</sup>
TTDPMLApYLQPFRRTS	1	pY <sup>1763</sup> L <sup>5</sup>
LESVYSLpYPTLSRLQ	1	pY <sup>2170</sup> P <sup>5</sup>
NLp <u>S</u> DIDQSFDK	1	pS <sup>2996</sup> D <sup>5,6,7,8</sup>

<sup>1</sup> Matsuoka et al (51); <sup>2</sup> Kozlov et al (36); <sup>3</sup> Bakkenist and Kastan 2003 (14); <sup>4</sup> Beausoleil et al (52); <sup>5</sup> <http://www.phosphosite.org> <sup>6</sup> Reported here <sup>7</sup> Shiloh et al (in press) <sup>8</sup> Daub et al (50)  
Underlined phosphorylation sites were manually confirmed.

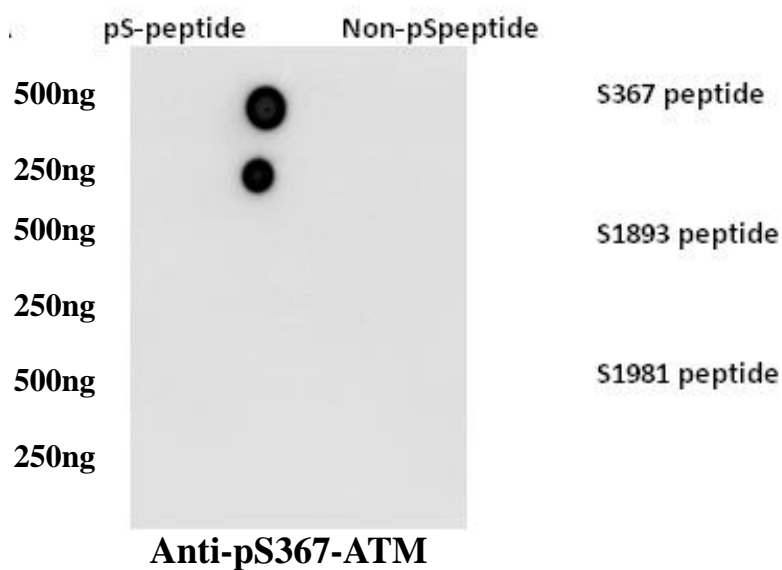


**C****D**

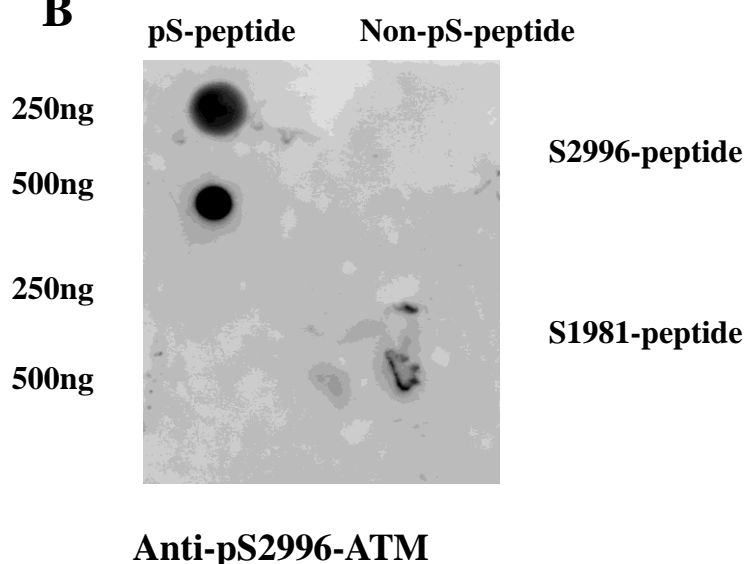
**E****F**

## Supplementary Figure 2

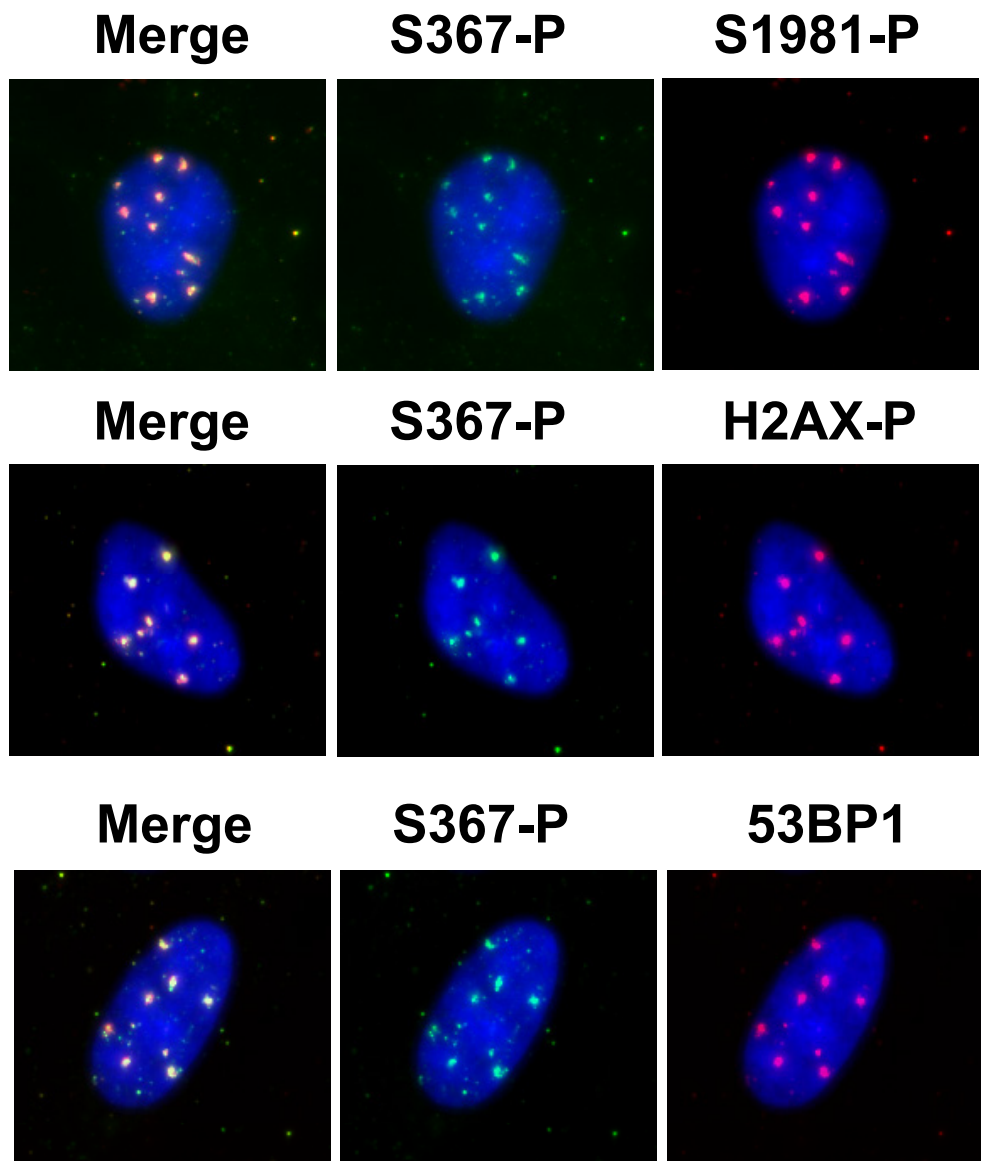
A



B

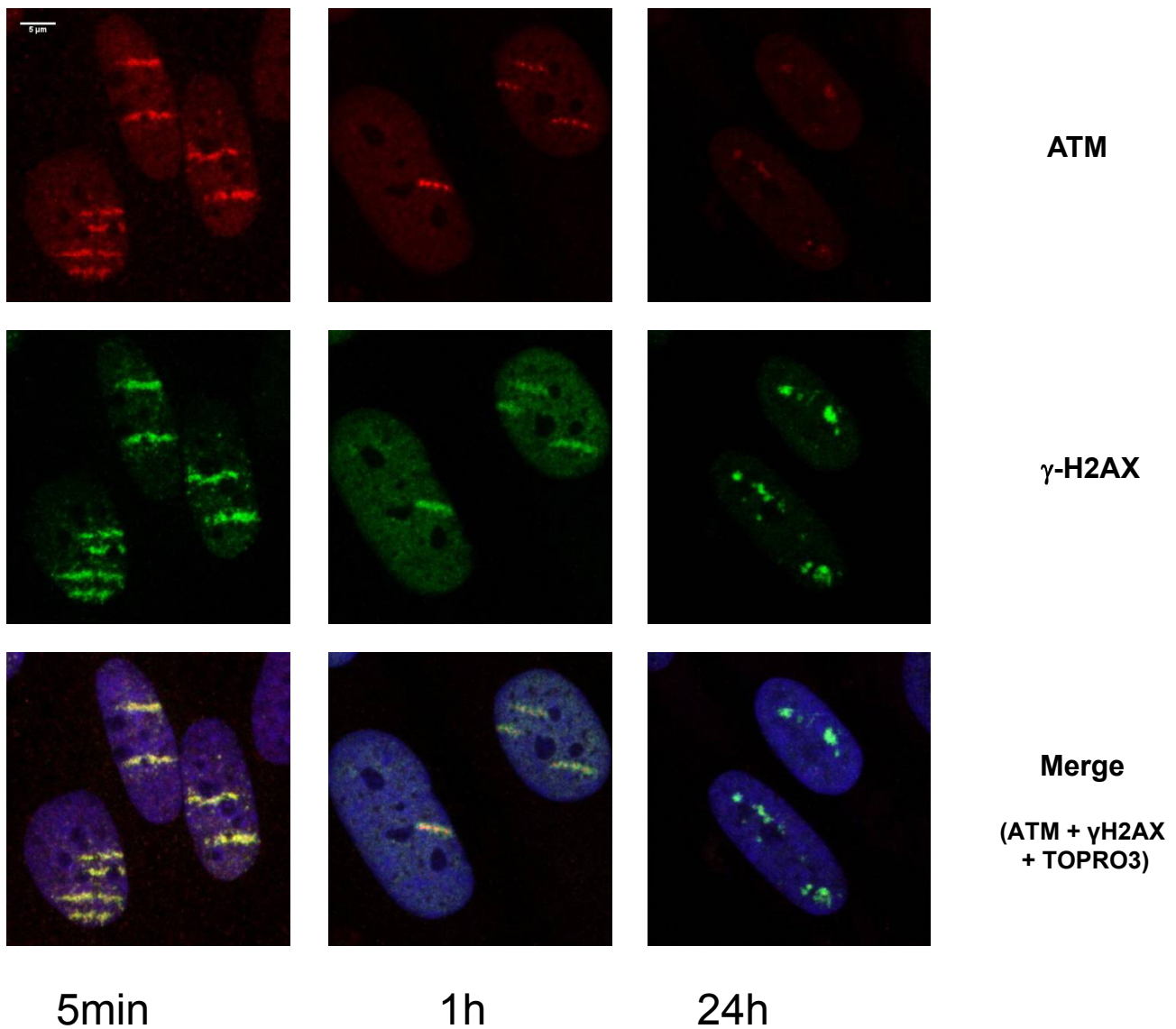


### Supplementary Figure 3

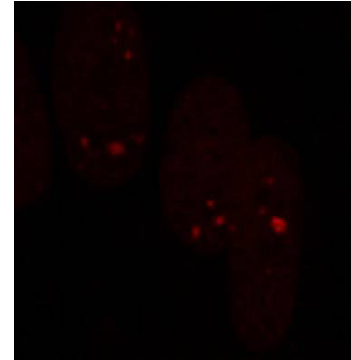
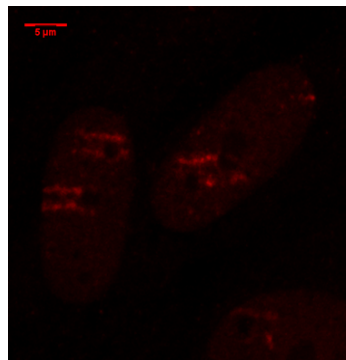


## Supplementary Figure 4

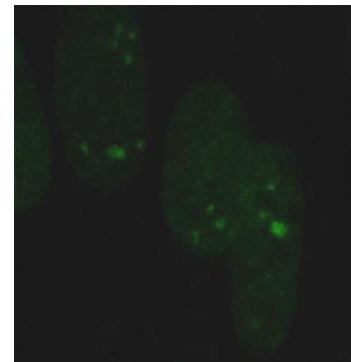
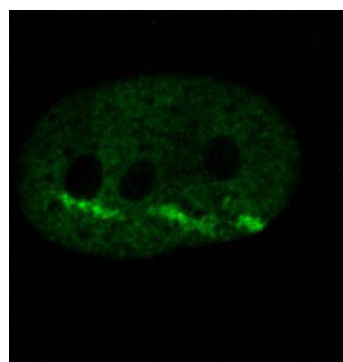
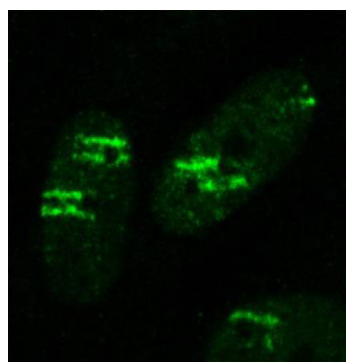
A



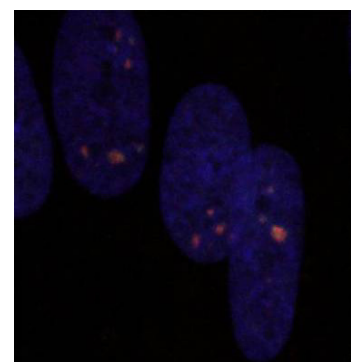
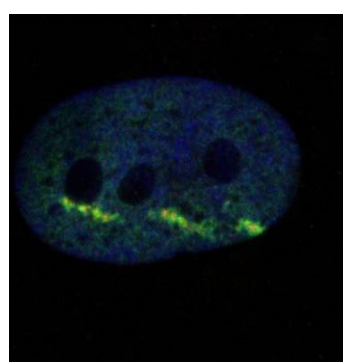
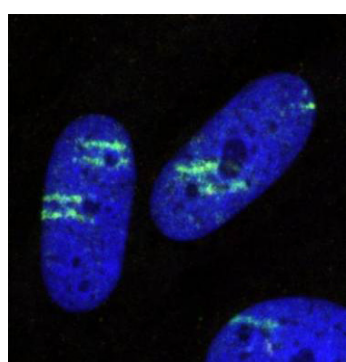
**B**



ATM pS1981



γ-H2AX



Merge

(ATM pS1981 + γH2AX  
+ TOPRO3)

5min

1h

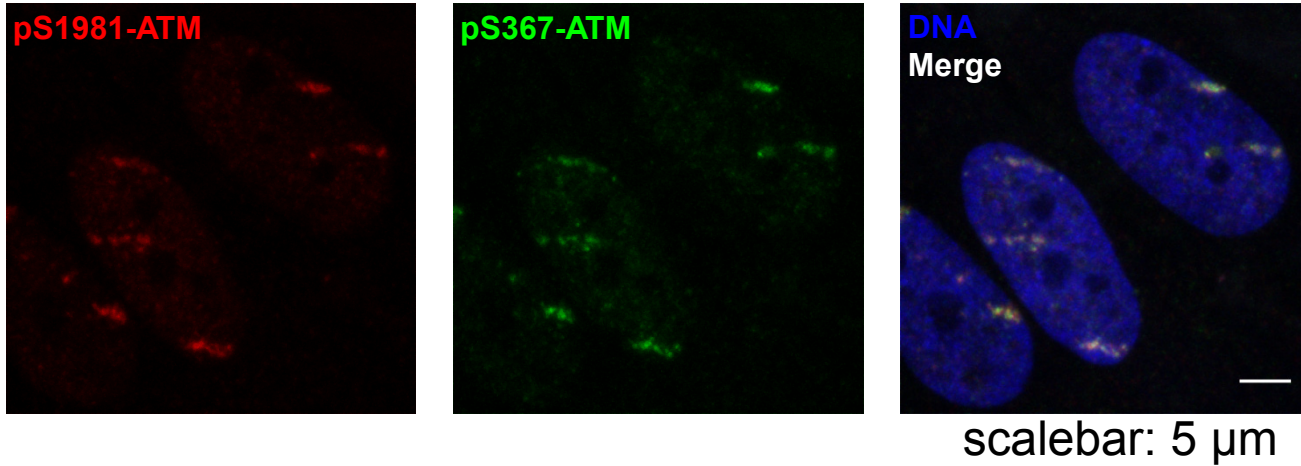
24h

## Supplementary Figure 5

A

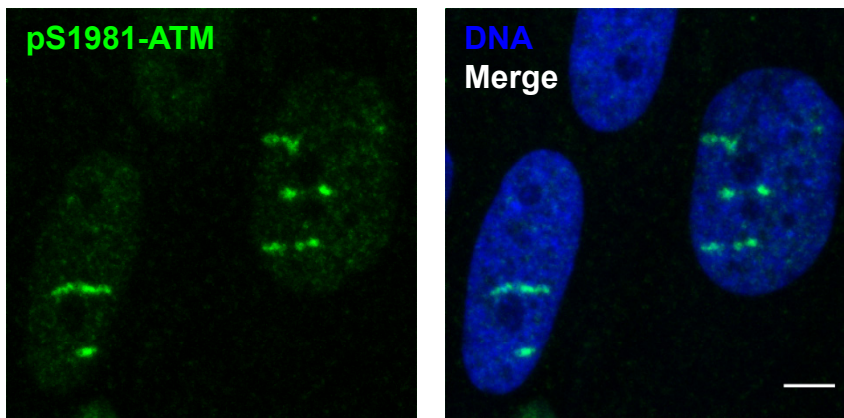


B



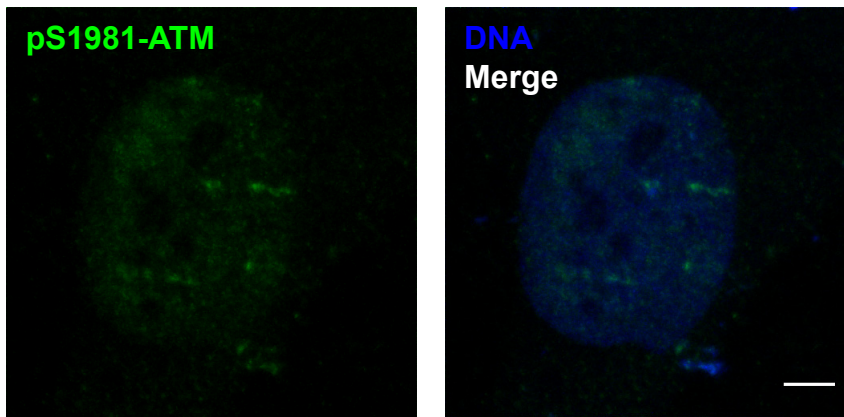
## Supplementary Figure 6

A



Control

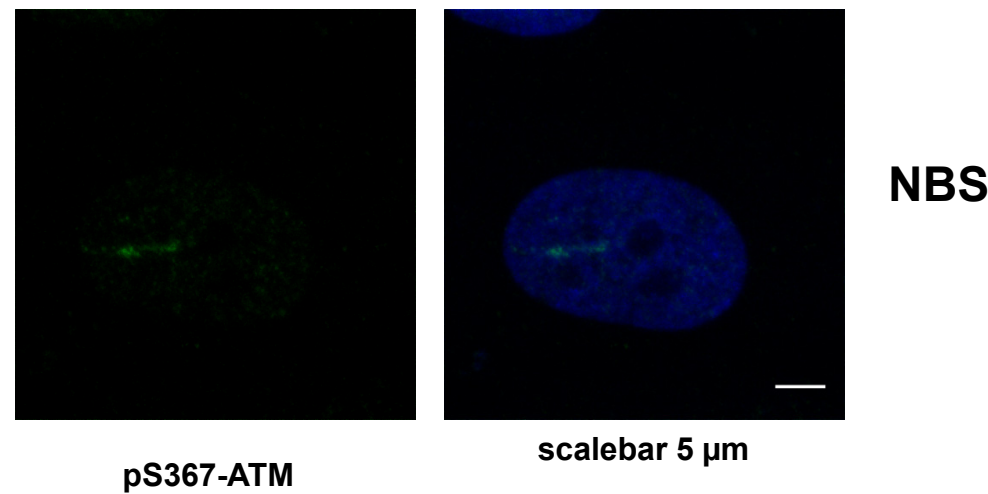
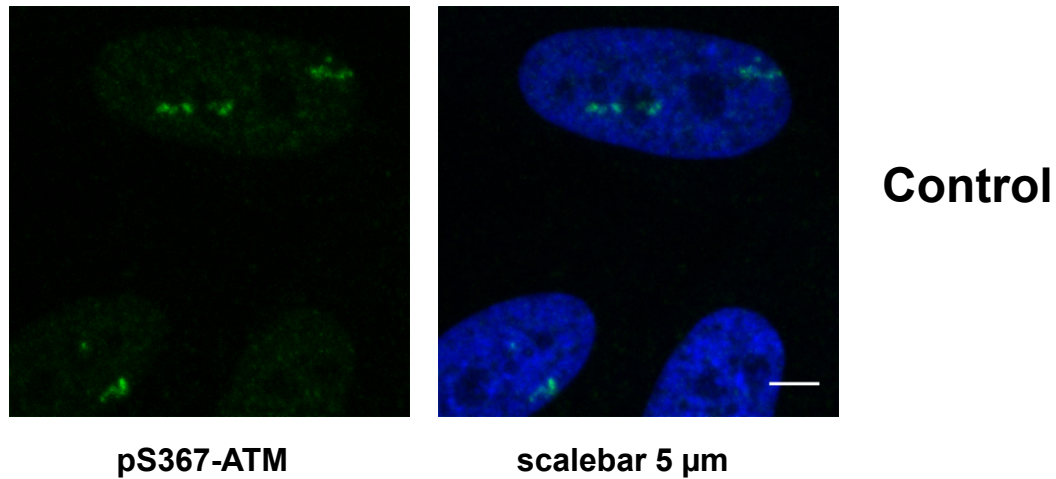
scalebar 5 μm



NBS

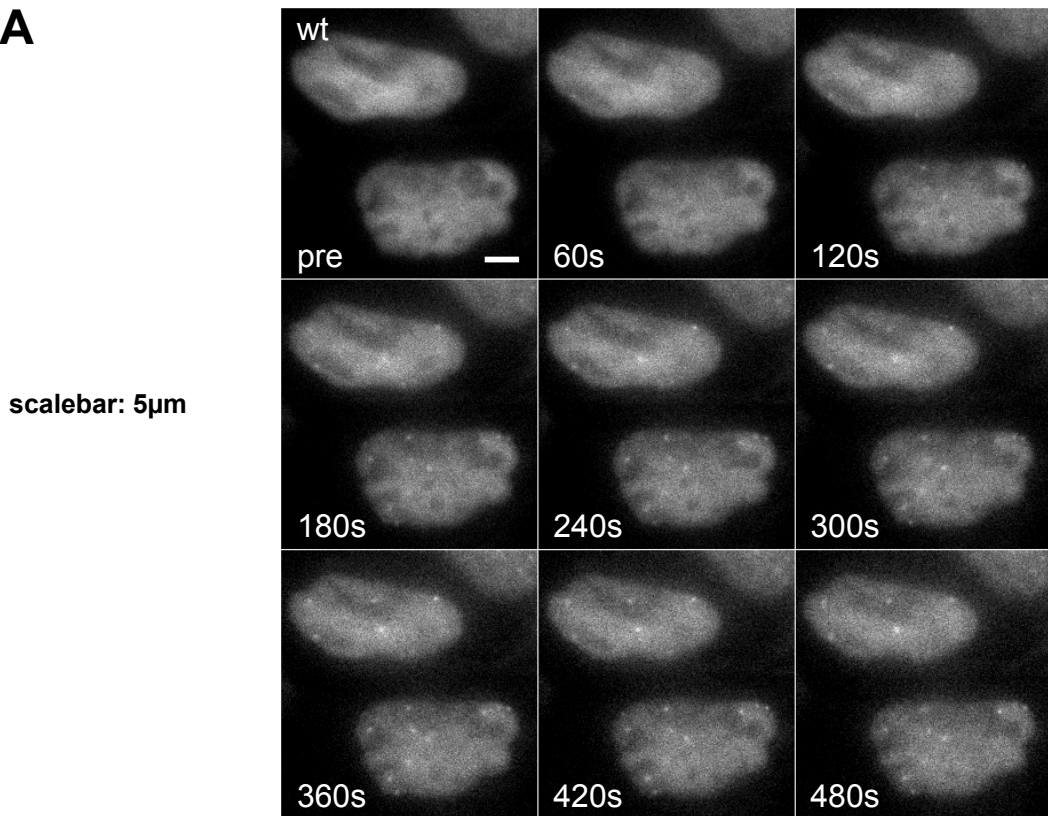
scalebar 5 μm

**B**



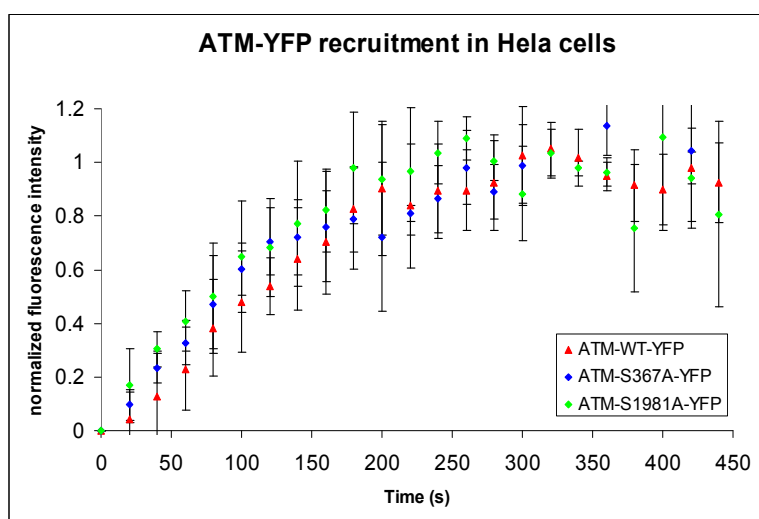
## Supplementary Figure 7

**A**



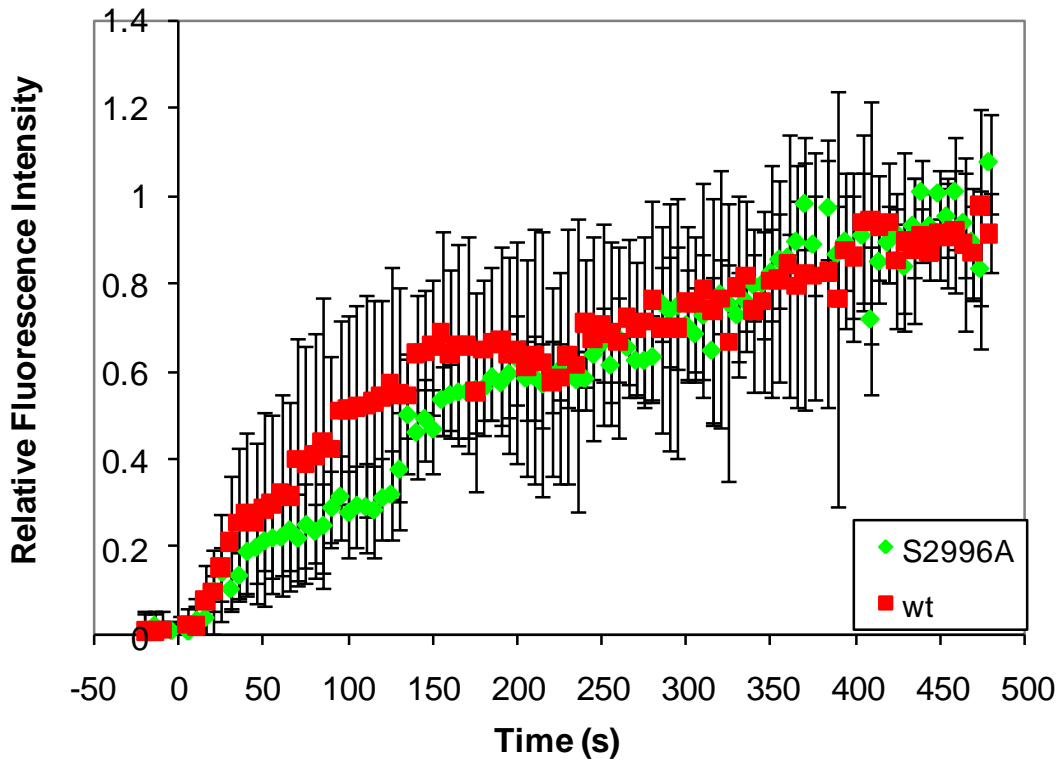
scalebar: 5μm

**B**



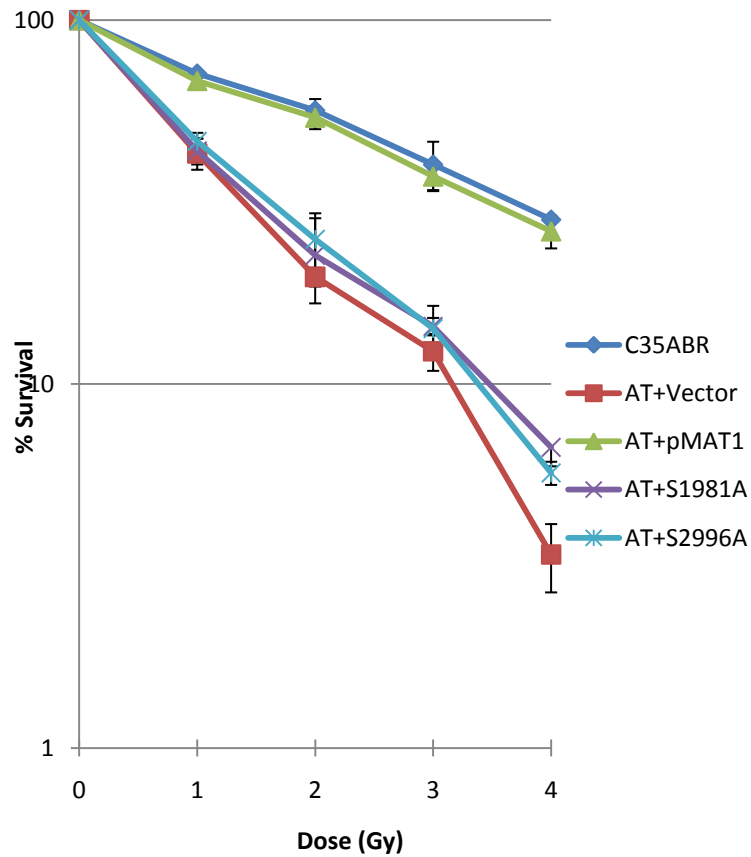
## Supplementary Figure 8

YFP-ATM-S2996A recruitment (gold ions)



## Supplementary Figure 9

A



B

